Evaluating the impact of assimilating CALIOP-derived aerosol extinction profiles on a global mass transport model

Jianglong Zhang,[1] James R. Campbell,[2] Jeffrey S. Reid,[2] Douglas L. Westphal,[2] Nancy L. Baker,[2] William F. Campbell,[2] and Edward J. Hyer[2]

Received 11 April 2011; revised 3 June 2011; accepted 5 June 2011; published 16 July 2011.

[1] Coupled two/three-dimensional variational (2D/3DVAR) assimilation of aerosol physical properties retrieved from the Moderate Resolution Imaging Spectroradiometer (MODIS), Multi-angle Imaging Spectroradiometer (MISR) and Cloud Aerosol Lidar with Orthogonal Polarization (CALIOP) satellite-borne instruments is described for the U. S. Navy Aerosol Analysis and Prediction System (NAAPS) global aerosol mass transport model. Coupled 2D/3DVAR assimilation for NAAPS is evaluated for 48-hr forecast cycles, computed four times daily in six-hour intervals, versus stand-alone 2DVAR assimilation of MODIS and MISR aerosol optical depths (AOD). Both systems are validated against AERONET ground-based sun photometer measurements of AOD. Despite a narrow nadir viewing swath and more than 2700 km of equatorial separation between orbits, satellite lidar data assimilation elicits a positive model response. Improvements in analysis and forecast AOD absolute errors are found over both land and maritime AERONET sites. The primary impact to the model from 3DVAR assimilation is the redistribution of aerosol mass into the boundary layer, though the process is sensitive to parameterization of vertical error correlation lengths. **Citation:** Zhang, J., J. R. Campbell, J. S. Reid, D. L. Westphal, N. L. Baker, W. F. Campbell, and E. J. Hyer (2011), Evaluating the impact of assimilating CALIOP-derived aerosol extinction profiles on a global mass transport model, *Geophys. Res. Lett.*, *38*, L14801, doi:10.1029/2011GL047737.

1. Introduction

[2] With recent advances in space-borne and ground-based observation platforms [e.g., *Holben et al.*, 1998; *Remer et al.*, 2008; *Kahn et al.*, 2010; *Winker et al.*, 2010], numerical forecast models of global aerosol distribution now benefit from data assimilation [*Zhang et al.*, 2008; *Uno et al.*, 2008; *Benedetti et al.*, 2009]. For example, the first operational aerosol data assimilation system, the *Navy Atmospheric Variational Data Assimilation System* (NAVDAS) *Aerosol Optical Depth* (NAVDAS-AOD), has been adopted by the *United States* (U.S.) *Navy Fleet Numerical Meteorology and Oceanography Center* (FNMOC) [*Zhang et al.*, 2008]. NAVDAS-AOD is based on the two-dimensional variational (2DVAR; x, y) version of the NRL Atmospheric Variational Data Assimilation System (NAVDAS) that processes quality-assured 2D satellite aerosol products [*Zhang et al.*, 2005; *Zhang and Reid*, 2006, 2009; *Hyer et al.*, 2011; *Shi et al.*, 2011]. Techniques optimizing column-integrated aerosol data assimilation via 2DVAR and 3DVAR (x, y, z) methods have been reported [e.g., *Weaver et al.*, 2007; *Zhang et al.*, 2008]. Further developments offer new promise for 4DVAR (x, y, z, t) assimilation of either 2D satellite aerosol optical depth retrievals [e.g., *Benedetti et al.*, 2009] or vertical lidar-derived extinction coefficient profiles [e.g., *Yumimoto et al.*, 2008; *Uno et al.*, 2008], and for 4D ensemble Kalman filter assimilation of ground-based measurements [e.g., *Schutgens et al.*, 2010] and lidar data [e.g., *Sekiyama et al.*, 2010].

[3] Datasets collected with the Cloud Aerosol Lidar with Orthogonal Polarization (CALIOP) instrument flown aboard the National Aeronautics and Space Administration (NASA) Cloud-Aerosol Lidar and Infrared Pathfinder Satellite Observation (CALIPSO) satellite [*Winker et al.*, 2009] exhibit great potential for constraining the vertical aerosol distribution in aerosol transport models. This paper thus considers a series of experiments designed for evaluating whether assimilating extinction coefficient profiles derived from CALIOP, with a limited near nadir-pointing swath and 2752.0 km equatorial separation between consecutive orbital passes, can improve global aerosol transport modeling and prediction. *Anderson et al.* [2003] suggest that horizontal covariance of aerosol physical properties exhibit a mean e-folding distance mean of only a few hundred kilometers, which was subsequently verified in satellite observations by *Zhang et al.* [2008]. 2DVAR methods alone, however, are incapable of directly reducing errors in the modeled vertical aerosol distribution. The expense of a 00-hr model analysis with inaccurate vertical resolution of aerosol mass is error downwind, since forecast trajectories diverge with height and time. Therefore, we integrate passive (e.g., MODIS and MISR) and active (e.g., CALIOP) aerosol data assimilation systems using coupled 2D/3DVAR versions of NAVDAS-AOD, and evaluate *U.S. Navy Aerosol Analysis and Prediction System* (NAAPS) model response versus 2DVAR-only forecasts of global AOD.

2. Methodology

[4] NAAPS is a 1° × 1° global aerosol mass transport model that computes 6-day forecasts of smoke, dust, sulfate, sea salt and SO_2 mass concentration every six hours. NAAPS is driven by dynamic fields generated by the *U. S. Navy Operational Global Analysis and Prediction System* [NOGAPS; *Hogan and Rosmond*, 1991]. NAAPS features a forward-scattering electro-optical propagation sub-system for native radiative transfer calculations [*Zhang et al.*, 2008],

[1]Department of Atmospheric Science, University of North Dakota, Grand Forks, North Dakota, USA.
[2]Marine Meteorology Division, Naval Research Laboratory, Monterey, California, USA.

Copyright 2011 by the American Geophysical Union.
0094-8276/11/2011GL047737

which considers hygroscopicity and ambient relative humidity for relating aerosol mass concentration and the extinction coefficient. Details on NAAPS and its source functions are given by *Reid et al.* [2009] for smoke, *Christensen* [1997] for sulfate, *Witek et al.* [2007] for sea salt, and *Westphal et al.* [1987], *Uno et al.* [2006] and *Walker et al.* [2009] for dust. Descriptions of the 2DVAR data assimilation system and its impact on system performance are given by *Zhang et al.* [2008] and *Reid et al.* [2009]. Global AOD analyses derived with NAAPS after 2DVAR assimilation of MODIS and MISR data, and validated using Level 2 (e.g., quality assured) *Aerosol Robotic Network* measurements (AERONET) [*Holben et al.*, 1998], exhibit accuracies comparable to that of satellite retrievals [e.g., *Zhang et al.*, 2008; *Zhang and Reid*, 2010; *Hyer et al.*, 2011]. NAAPS forecasts are improved by 20–40% for both over land and over ocean AOD assimilation [*Zhang et al.*, 2008, 2010].

[5] The NAVDAS-AOD paradigm for coupled 2D/3DVAR NAAPS data assimilation using MODIS/MISR and CALIOP is summarized as follows:

[6] 1. Create an AOD 00-hr analysis by assimilating quality-assured MODIS and MISR AOD products with the valid NAAPS 06-hr forecast using the 2DVAR version of NAVDAS-AOD [*Zhang et al.*, 2008]; convert into a first-guess 3D analysis of aerosol mass concentration and extinction coefficient.

[7] 2. Use this AOD analysis to constrain and derive CALIOP aerosol extinction coefficient profiles [*Campbell et al.*, 2010].

[8] 3. Perform 3DVAR assimilation of the profiles; use the 3D extinction analysis to produce a final 3D mass concentration field.

[9] 4. Run NAAPS in forecast mode out to 48 hours.

[10] 5. Repeat steps 1–4 for time +06 hr.

[11] Quality-screened MODIS over-ocean [*Zhang and Reid*, 2006; *Shi et al.*, 2011] and over-land AOD [*Hyer et al.*, 2011] products and Version 1 of an assimilation-grade MISR AOD product [*Shi*, 2009] have been described. CALIOP-derived 0.532 μm aerosol extinction coefficient profiles with corresponding uncertainties are generated during Step 2 using one-degree along-track averages of cloud-cleared signal profiles collected between 60°S–60°N that are assigned to the closest NAAPS grid point [*Campbell et al.*, 2010]. An 'observed' aerosol extinction coefficient profile is iteratively derived from these data using a numerical inversion technique that is constrained by the model AOD solved at Step 2 (AOD_{2DVAR}). Hence, this 'observed' profile and the first-guess extinction coefficient profile from the model for the same grid point have the same value of vertically-integrated extinction (i.e., AOD_{2DVAR}). Derivation of the "lidar ratio" (the layer-mean aerosol extinction-to-backscatter ratio), a by-product of the numerical inversion, allows for screening questionable 'observations' that are likely cloud contaminated.

[12] At Step 3, error variance for the NAAPS extinction coefficient analysis generated from Step 1 is estimated by comparing with collocated CALIOP-derived extinction profiles at four pressure ranges: >900 hPa, 800–900 hPa, 700–800 hPa, and <700 hPa. A horizontal aerosol extinction coefficient error correlation length of 200.0 km is parameterized based on that of *Zhang et al.* [2008]. The vertical error correlation (R) at two pressure levels, p_1 and p_2, is estimated from a second order autoregressive function as

$$R = \left[1 + \left|\int_{p_1}^{p_2} \frac{d\ln p}{L}\right|\right] e^{-\left|\int_{p_1}^{p_2} \frac{d\ln p}{L}\right|}. \quad (1)$$

For our primary analysis, the vertical error correlation length (L) is fixed at 0.015 (unit less), or approximately 0.1 km if the scale height is set to 7.0 km. Error correlation between aerosol mass concentration and other potentially dependent meteorological parameters is presumed negligible, though such advanced prognostic error models are considered requisite for future model development via ensemble-based approaches [e.g., *Schutgens et al.*, 2010]. L varies as a function of altitude, time (e.g., season), and location (e.g., land versus ocean). Secondary experiments and investigation of model sensitivity to L are described in Section 3. Fixing L = 0.015 was found during testing to yield the most stable performance for primary model assessment.

[13] The model extinction coefficient profile derived from Step 3 does not yield the same vertical integral of extinction (i.e., AOD_{3DVAR}) as the assimilated one, as the weights assigned to the 'observation' and first-guess profiles are different. Weighting offsets occur when the observation or model is more trusted than the other for assimilation, or for grid points away from the CALIOP track where weights decrease based on correlation settings described above. If the weights were identical, then the vertical integral of extinction would be conserved and AOD_{3DVAR} would equal AOD_{2DVAR}. With relation to the profile of aerosol mass concentration solved from Step 3, the vertical redistribution of aerosol extinction caused by 3DVAR assimilation is sensitive to variations in humidity and thus aerosol hygroscopicity. Aerosol mass is not conserved during the 3DVAR process.

3. Results and Discussions

[14] Example output from various stages of the coupled 2D/3DVAR assimilation system is shown in Figure 1. Figure 1a depicts the CALIOP Level 1B 0.532 μm attenuated backscatter profile at the native 20.16 Hz pulse repetition frequency and 0.030/0.060 km vertical resolutions from 0.0 to 8.2/8.2–12.0 km above mean sea level (MSL), respectively, between 35° and 10°N for the 2122 UTC nighttime granule 17 May 2007. During this orbital segment, the satellite moved southwesterly off the Tibetan plateau, over Afghanistan and Pakistan, and then the northern Arabian Sea. Dust was profiled aloft, and enhanced backscatter signals at 2.0 km MSL were observed beginning near 33°N/70°E. A shallow low-level plume extends from 27°N to near the southern end of the segment shown. Between these two features, a slanting layer was profiled from 1.0 km MSL (25°N/70°E) to near 3.5 km MSL (20°N/70°E).

[15] Shown in Figure 1b are cloud-cleared CALIOP one-degree along-track averaged signal profiles, described above and solved as part of Step 2, now scaled between 0.0 and 8.0 km MSL. Superimposed on these data are layer boundaries derived using a feature-finding algorithm that discriminates particulate (i.e., aerosol particle) scattering from that of the molecular atmosphere [*Campbell et al.*, 2008].

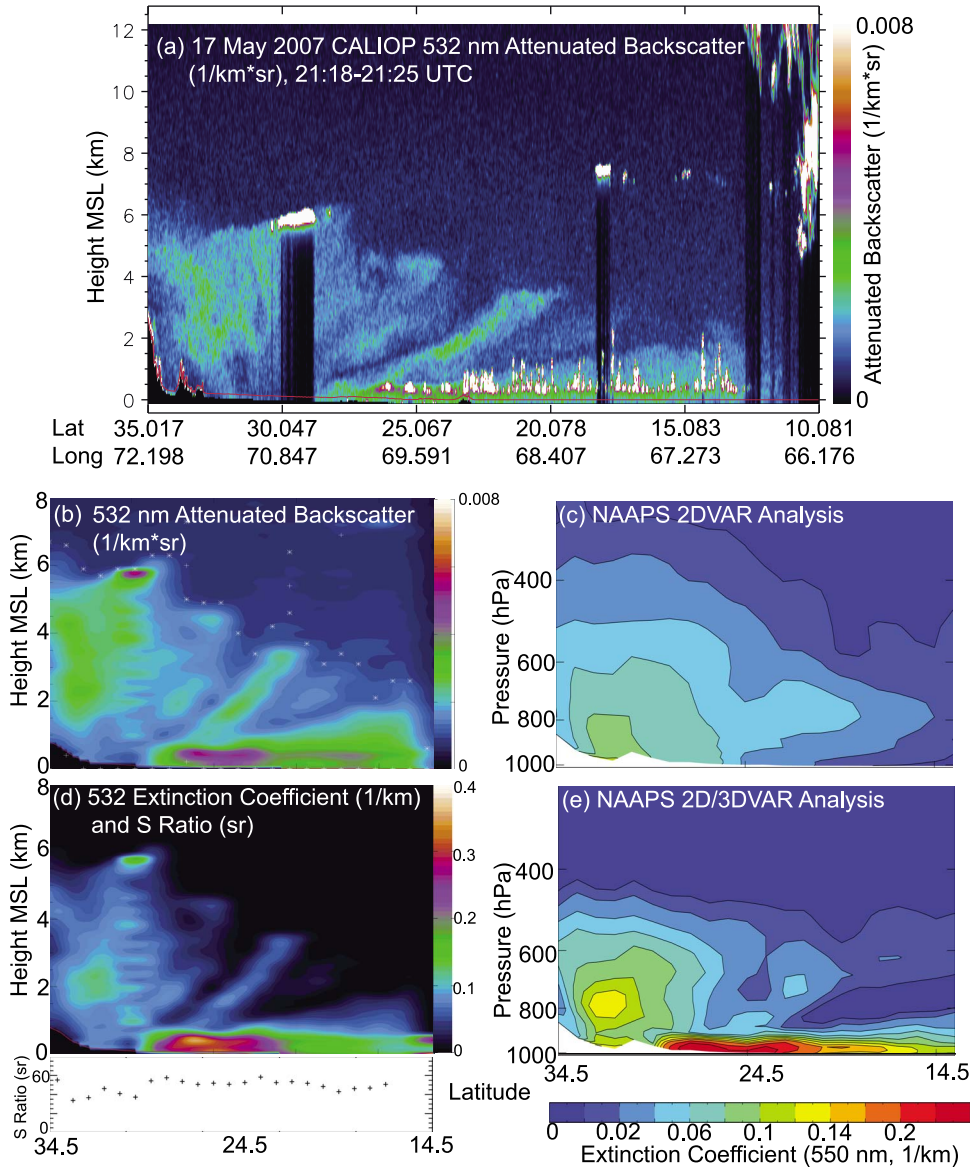

Figure 1. (a) CALIOP 0.532 μm attenuated backscatter (km^{-1} sr^{-1}) for 2122 UTC northeasterly orbital pass 17 May 2007, 35° to 10° N from 0.0 to 12.0 km MSL; (b) 1° along-track averaged and cloud-cleared attenuated backscatter profiles from 0.0 to 8.0 km MSL; (c) NAAPS analysis of extinction per model sigma level ($level^{-1}$) from 1000.0 to 300.0 hPa for this pass using only MODIS/MISR optical depth assimilation; (d) 0.532 μm extinction coefficient and extinction-to-backscatter ratios for inversion constrained by NAAPS optical depths in Figure 1c; (e) NAAPS analysis post-CALIOP assimilation. Derived aerosol layer top and bottom heights for the inversion step are shown in Figure 1b using asterisks and plus symbols, respectively.

Shown in Figure 1c is the NAAPS 00-hour model analysis at 0000 UTC 18 May 2007 of the 550 nm aerosol extinction coefficient from 1000.0 to 100.0 hPa, corresponding with the CALIPSO coordinates in Figure 1a. The model predicted a dust layer from 20°–35°N, but failed to resolve the near-surface layer between 27°–13°N. Shown in Figure 1d are CALIOP-derived retrievals of the aerosol extinction coefficient, again from Step 2. Conversion between 550 and 532 nm is done using a simple Angstrom exponent relationship predicated on the spectral AOD solved within NAAPS. Calculations of the pre-cursor "lidar ratio" step are shown in the inset of Figure 1d. The NAAPS reanalysis of 550 nm extinction coefficient is shown in Figure 1e after 3DVAR assimilation in Step 3. The vertical redistribution of aerosol particle mass is apparent, and represents a more accurate depiction of the layers profiled by CALIOP.

[16] Figure 2a depicts the difference between NAAPS and AERONET for AOD forecasts in 06-hr intervals out to 48 hr derived using NAVDAS-AOD 2DVAR alone and the coupled 2D/3DVAR system, respectively. These results were derived using spatially and temporally collocated NAAPS and AERONET data. We require AERONET observations to be within ±30 minutes of the NAAPS forecast time, and use the closest NAAPS grid point to the AERONET site (within ±1° Lat/Lon). Vertical lines represent the 95% confident interval for mean absolute error, and Gaussian

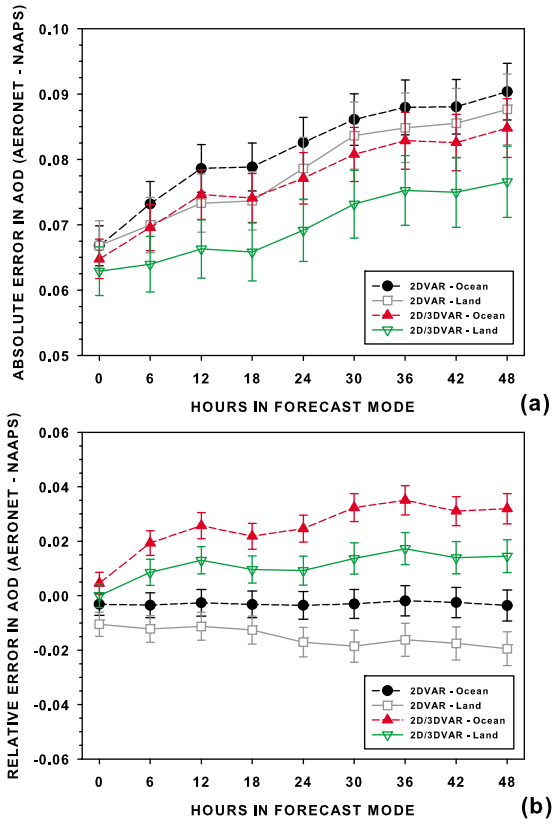

Figure 2. (a) Two month (June–July 2007) averaged absolute AOD error for NAAPS 2DVAR versus coupled 2D/3DVAR assimilation, solved versus AERONET as a function of forecast length both over ocean (coastal and island sites) and over land, respectively (see inset). Vertical lines represent the 95% confident interval for the mean absolute error, assuming a Gaussian data distribution. (b) Similar to Figure 2a but for the averaged relative AOD error.

distributions were assumed for all datasets. 48-hr runs were conducted during June–July 2007 at 00, 06, 12 and 18 UTC, with forecasts predicated on NOGAPS reanalysis meteorological fields. The coupled 2D/3DVAR system was run for two weeks prior to 1 June in order to stabilize the model for evaluation. Differences in error between the two systems thus represent both the instantaneous effect of data assimilation and the accumulated improvement to the analysis having occurred progressively upstream. Comparisons were separated into over land and ocean cases for both systems. Improvements in absolute error for the coupled system were found in both cases. More than 10% improvement was found for the over-land case. Improvement is less over oceans. We attribute this difference to the relative stability of the vertical aerosol distribution for transport events over large water bodies, in contrast to over land and in relatively closer proximity to source regions.

[17] The relative offset in absolute errors solved at the 12 and 36-hr steps for each of the profiles shown in Figure 2a is due to the non-linear influence of two inherent system processes. The first involves the 180° phase difference between data availability in one global quadrant of the model for assimilation at 00-hr where the sun is overhead (MODIS, MISR, and CALIOP) versus these specific forecast validation times when AERONET data become available but whose sectors were shroud in darkness at initialization (CALIOP data assimilated only). Second, differences in AERONET AOD data availability and instrument distributions within the quadrants cause systematic variability in derived errors.

[18] Figure 2b depicts a similar analysis as Figure 2a, but instead for relative error solved between AERONET and the NAAPS assimilation systems. For 2DVAR alone, NAAPS forecasts over-estimate AOD by less than 0.01 over ocean and 0.01–0.02 over land. In contrast, AOD is under-estimated by 0.02–0.03 over ocean and 0.01–0.02 over land when coupled 2D/3DVAR is run. This result reflects current NAAPS particle deposition parameterizations and their sensitivities [e.g., *Xian et al.*, 2009]. As shown in Figure 1, and discussed further below, coupled 2D/3DVAR assimilation primarily causes particle redistribution from the free troposphere into the boundary layer, where deposition occurs. Therefore, mass is increasingly subject to removal from the model over the forecast interval, which is depicted as an increasing offset over time.

[19] Figure 3a depicts the averaged difference between CALIOP observation and corresponding NAAPS 00-hr analysis extinction profiles after 2DVAR and the coupled 2D/3DVAR runs over both land and ocean, respectively (observation minus analyses, O-A, where the 'observation' represents the result of Step 2 described above). Without CALIOP assimilation, NAAPS underestimates aerosol mass concentration near the surface. This effect is most pronounced over oceans, perhaps suggesting scavenging in the marine boundary layer. Previous field research has identified similar weaknesses in model parameterizations at the lower boundary [e.g., *Colarco et al.*, 2003; *Reid et al.*, 2003]. After assimilating CALIOP data however, mass concentrations near the surface layer are increased. A bi-modal structure is seen in the coupled 2D/3DVAR O-A profile. Use of a fixed setting for L is the primary deterministic factor influencing this result. However, secondary factors also impact this finding. First, a single assimilation step yields only intermediate convergence to a given CALIOP observation. Second, differences in resolution between the lidar profile and the depth of the sigma levels used within the model, which increase with height, can bias the vertical redistribution of aerosol mass caused by assimilation.

[20] Shown in Figure 3b are differences between CALIOP and NAAPS extinction profiles for the 06-hr forecast (observation minus forecasts; O-F), again for both 2DVAR and coupled 2D/3DVAR assimilation over both land and oceans, respectively. We use what become the assimilated CALIOP profiles when the model is reinitialized six hours later in order to have observations available for the +06 hour forecast time. Further, note that the last time this region of the model was impacted by CALIOP assimilation is at least twelve hours prior, depending on latitude, since CALIPSO orbital tracks intersect each quadrant of the model every six hours. Still, the results in Figure 3b are very similar to those described from Figure 3a; the primary impact of CALIOP assimilation is the redistribution of aerosol mass into the boundary layer.

[21] Figure 3c depicts coupled 2D/3DVAR system O-A profiles solved where L is varied from 0.015 at the surface and increasing to 0.045 by 450 hPa. Less fluctuation and improved convergence to zero are found throughout the model column, compared with corresponding results derived with a fixed L in Figure 3a. Similar improvement is found

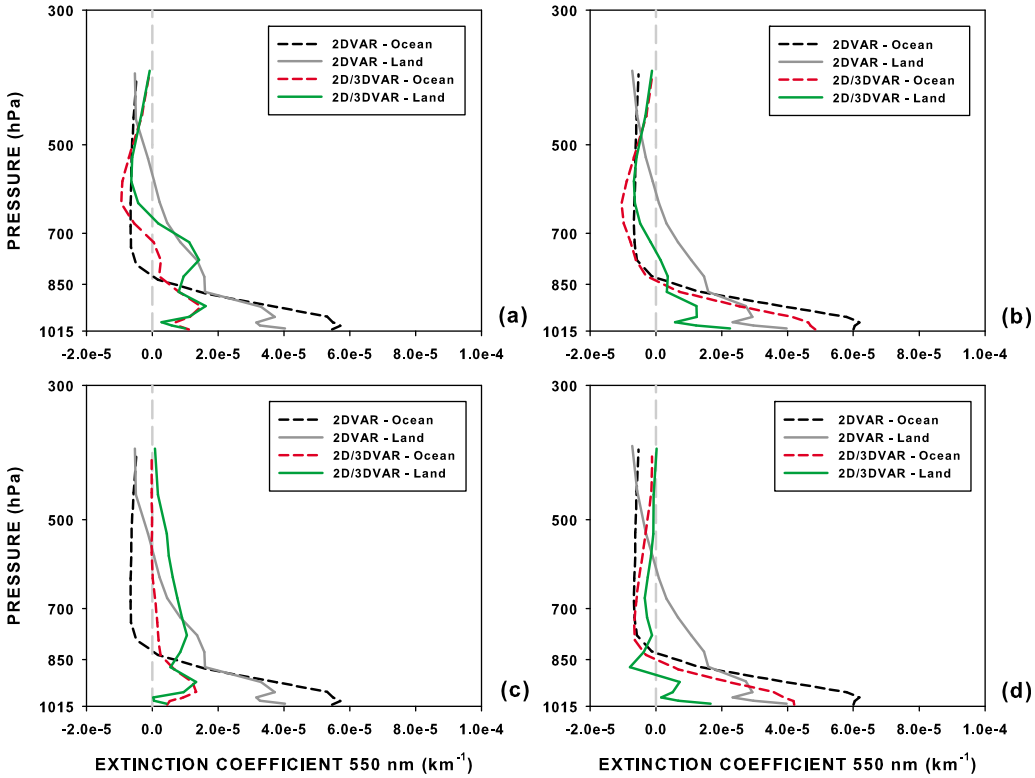

Figure 3. (a) Two month (June–July 2007) averaged CALIPSO minus NAAPS (analysis) extinction profiles (O-A) for both 2DVAR (red and green lines), and coupled 2D/3DVAR (grey and black lines) cases, over both land and oceans (see inset). (b) Similar to Figure 3a, but for the six-hour forecast (O-F). (c) Similar to Figure 3a, but for O-A using a variable vertical background error correlation length. (d) Similar to Figure 3b, but for O-F using a variable vertical background error correlation length.

from the coupled 2D/3DVAR O-F analysis (Figure 3d). It is physically realistic for L to increase with altitude. Applying a fixed L, however, aside from simplicity, still represents a reasonable model option. Since CALIOP-derived extinction profiles are constrained by AOD_{2DVAR}, they are correlated with NAAPS extinction profiles solved at Step 1. Therefore, varying L may induce a loss of aerosol mass, as larger values are assigned to high altitudes where aerosol concentrations are low. Second, L very likely varies with region (particularly with respect to land versus ocean) and diurnal cycle, for which a robust parameterization is presently unavailable. These findings ultimately indicate, however, how the model, and its apparent improvement, are sensitive to L, for which we conclude a more thorough assessment and 3D prognostic error model be considered as part of future model upgrades.

4. Conclusions and Implications

[22] Using two months of satellite aerosol observations from MODIS, MISR and CALIOP, we evaluate a coupled two/three-dimensional variational data assimilation (2D/3DVAR) system using the *U.S. Navy Aerosol Analysis and Prediction System* (NAAPS) global mass transport model. NAAPS analysis fields derived from 2DVAR MODIS and MISR assimilation are used to constrain retrievals predicated on CALIOP data in order to derive 1° × 1° gridded and cloud-free aerosol extinction profiles. Coupled 2D/3DVAR assimilation improves the vertical representation of the 00-hr aerosol analysis state in NAAPS, which is interpreted from improved globally-averaged AOD solved throughout the 48-hr model forecast, as validated using *Aerosol Robotic Network* (AERONET) ground sun-photometer measurements and compared with 2DVAR assimilation alone. Improvement in model performance over land is greater than that over water. The primary impact of coupled 2D/3DVAR assimilation is the redistribution of aerosol mass into the model boundary layer. However, this result is sensitive to parameterization of the vertical error correlation length. The findings in this paper confirm that assimilation of CALIOP aerosol products is effective for improving forecasts of model AOD.

[23] With respect to a global numerical model run at single-degree horizontal resolution (i.e., 1° × 1°), data collected with a nadir-pointing polar-orbiting satellite lidar instrument is relatively coarse over all but the polar regions [*Campbell et al.*, 2010]. Nevertheless, the results described from Figure 2 illustrate that even with the limited CALIOP sensor swath [*Winker et al.*, 2010], and with parameterized 3D error correlation lengths (i.e., not solved using ensemble and/or Kalman filter techniques), a positive impact is made on the model. This is an encouraging result, which will only improve with future satellite lidar monitoring activities. Missions featuring high-spectral resolution measurements [e.g., *Grund and Eloranta*, 1991] and a direct retrieval of the aerosol extinction coefficient would simplify the coupled 2D/3DVAR paradigm. Furthermore, a 3D prognostic error model is being developed for the coupled 2D/3DVAR NAAPS system using ground-based lidar validation that will

optimize error correlation settings. The attention of mission planners, science teams and investigators tasked with raising the visibility of satellite lidar aerosol datasets for global aerosol visibility forecasting is vital to ensuring that these endeavors are pursued until operational status is attained. This paper represents a demonstration of potential, viability and system development necessary to achieve this goal.

[24] **Acknowledgments.** This research was funded by the Office of Naval Research Code 32, the Office of Naval Research Young Investigator Program, and the NASA Interdisciplinary Science Program. Authors J.R.C. and J.S.R. acknowledge NASA grant NNH07AG44I as part of the CALIPSO Science Team. The group acknowledges the AERONET program, their contributing principal investigators and their staff for coordinating the coastal and inland sites used in this investigation.

[25] The Editor thanks two anonymous reviewers for their assistance in evaluating this paper.

References

Anderson, T. L., R. J. Charlson, D. M. Winker, J. A. Ogren, and K. Holmén (2003), Mesoscale variations of tropospheric aerosols, *J. Atmos. Sci.*, *60*, 119–136, doi:10.1175/1520-0469(2003)060<0119:MVOTA>2.0.CO;2.

Benedetti, A., et al. (2009), Aerosol analysis and forecast in the European Centre for Medium-Range Weather Forecasts Integrated Forecast System: 2. Data assimilation, *J. Geophys. Res.*, *114*, D13205, doi:10.1029/2008JD011115.

Campbell, J. R., K. Sassen, and E. J. Welton (2008), Elevated cloud and aerosol layer retrievals from micropulse lidar signal profiles, *J. Atmos. Oceanic Technol.*, *25*, 685–700, doi:10.1175/2007JTECHA1034.1.

Campbell, J. R., J. S. Reid, D. L. Westphal, J. Zhang, E. J. Hyer, and E. J. Welton (2010), CALIOP aerosol subset processing for global aerosol transport model data assimilation, *IEEE J. Sel. Top. Appl. Earth Obs. Remote Sens.*, *3*, 203–214, doi:10.1109/JSTARS.2010.2044868.

Christensen, J. H. (1997), The Danish eulerian hemispheric model—A three-dimensional air pollution model used for the arctic, *Atmos. Environ.*, *31*, 4169–4191, doi:10.1016/S1352-2310(97)00264-1.

Colarco, P., et al. (2003), Saharan dust transport to the Caribbean during PRIDE: 2. Transport, vertical profiles, and deposition in simulations of in situ and remote sensing observations, *J. Geophys. Res.*, *108*(D19), 8590, doi:10.1029/2002JD002659.

Grund, C. J., and E. W. Eloranta (1991), University of Wisconsin high spectral resolution lidar, *Opt. Eng.*, *30*, 6–12, doi:10.1117/12.55766.

Hogan, T. F., and T. E. Rosmond (1991), The description of the Navy Operational Global Atmospheric Prediction Systems spectral forecast model, *Mon. Weather Rev.*, *119*, 1786–1815, doi:10.1175/1520-0493(1991)119<1786:TDOTNO>2.0.CO;2.

Holben, B. N., et al. (1998), AERONET—A federated instrument network and data archive for aerosol characterization, *Remote Sens. Environ.*, *66*, 1–16, doi:10.1016/S0034-4257(98)00031-5.

Hyer, E. J., J. S. Reid, and J. Zhang (2011), An over-land aerosol optical depth data set for data assimilation by filtering, correction, and aggregation of MODIS Collection 5 optical depth retrievals, *Atmos. Meas. Tech.*, *4*, 379–408, doi:10.5194/amt-4-379-2011.

Kahn, R. A., B. J. Gaitley, M. J. Garay, D. J. Diner, T. Eck, A. Smirnov, and B. N. Holben (2010), MISR aerosol product assessment by comparison with AERONET, *J. Geophys. Res.*, *115*, D23209, doi:10.1029/2010JD014601.

Reid, J. S., et al. (2003), Analysis of measurements of Saharan dust by airborne and ground-based remote sensing methods during the Puerto Rico Dust Experiment (PRIDE), *J. Geophys. Res.*, *108*(D19), 8586, doi:10.1029/2002JD002493.

Reid, J. S., et al. (2009), Global monitoring and forecasting of biomass-burning smoke: Description of and lessons from the Fire Locating and Modeling of Burning Emissions (FLAMBE) program, *IEEE J. Sel. Top. Appl. Earth Obs. Remote Sens.*, *2*, 144–162, doi:10.1109/JSTARS.2009.2027443.

Remer, L. A., et al. (2008), Global aerosol climatology from the MODIS satellite sensors, *J. Geophys. Res.*, *113*, D14S07, doi:10.1029/2007JD009661.

Schutgens, N. A. J., T. Miyoshi, T. Takemura, and T. Nakajima (2010), applying an ensemble Kalman filter to the assimilation of AERONET observations in a global aerosol transport model, *Atmos. Chem. Phys.*, *10*, 2561–2576, doi:10.5194/acp-10-2561-2010.

Sekiyama, T. T., T. Y. Tanaka, A. Shimizu, and T. Miyoshi (2010), Data assimilation of CALIPSO aerosol observations, *Atmos. Chem. Phys.*, *10*, 39–49, doi:10.5194/acp-10-39-2010.

Shi, Y. (2009), Development of data-assimilation-quality MODIS and MISR over water aerosol products, M.S. thesis, 74 pp., Dep. of Atmos. Sci., Univ. of N. D., Grand Forks.

Shi, Y., J. Zhang, J. S. Reid, B. Holben, E. J. Hyer, and C. Curtis (2011), An analysis of the collection 5 MODIS over-ocean aerosol optical depth product for its implication in aerosol assimilation, *Atmos. Chem. Phys.*, *11*, 557–565, doi:10.5194/acp-11-557-2011.

Uno, I., et al. (2006), Dust model intercomparison (DMIP) study over Asia: Overview, *J. Geophys. Res.*, *111*, D12213, doi:10.1029/2005JD006575.

Uno, I., K. Yumimoto, A. Shimizu, Y. Hara, N. Sugimoto, Z. Wang, Z. Liu, and D. M. Winker (2008), 3D structure of Asian dust transport revealed by CALIPSO lidar and a 4DVAR dust model, *Geophys. Res. Lett.*, *35*, L06803, doi:10.1029/2007GL032329.

Walker, A. L., M. Liu, S. D. Miller, K. A. Richardson, and D. L. Westphal (2009), Development of a dust source database for mesoscale forecasting in southwest Asia, *J. Geophys. Res.*, *114*, D18207, doi:10.1029/2008JD011541.

Weaver, C., A. da Silva, M. Chin, P. Ginoux, O. Dubovik, D. Flittner, A. Zia, L. Remer, B. Holben, and W. Gregg (2007), Direct insertion of MODIS radiances in a global aerosol transport model, *J. Atmos. Sci.*, *64*, 808–827, doi:10.1175/JAS3838.1.

Westphal, D. L., O. B. Toon, and T. N. Carlson (1987), A two-dimensional numerical investigation of the dynamics and microphysics of Saharan dust storms, *J. Geophys. Res.*, *92*, 3027–3049, doi:10.1029/JD092iD03p03027.

Winker, D. M., M. A. Vaughan, A. Omar, Y. Hu, K. A. Powell, Z. Liu, W. H. Hunt, and S. A. Young (2009), Overview of the CALIPSO mission and CALIOP data processing algorithms, *J. Atmos. Oceanic Technol.*, *26*, 2310–2323, doi:10.1175/2009JTECHA1281.1.

Winker, D. M., et al. (2010), The CALIPSO mission: A global 3D view of aerosols and clouds, *Bull. Am. Meteorol. Soc.*, *91*, 1211–1229, doi:10.1175/2010BAMS3009.1.

Witek, M., P. J. Flatau, P. K. Quinn, and D. L. Westphal (2007), Global sea-salt modeling: Results and validation against multi-campaign shipboard measurements, *J. Geophys. Res.*, *112*, D08215, doi:10.1029/2006JD007779.

Xian, P., J. S. Reid, J. F. Turk, E. J. Hyer, and D. l. Westphal (2009), Impact of modeled versus satellite measured tropical precipitation on regional smoke optical thickness in an aerosol transport model, *Geophys. Res. Lett.*, *36*, L16805, doi:10.1029/2009GL038823.

Yumimoto, K., I. Uno, N. Sugimoto, A. Shimizu, Z. Liu, and D. M. Winker (2008), Adjoint inversion modeling of Asian dust emission using lidar observations, *Atmos. Chem. Phys.*, *8*, 2869–2884, doi:10.5194/acp-8-2869-2008.

Zhang, J., and J. S. Reid (2006), MODIS Aerosol Product Analysis for Data Assimilation: Assessment of Level 2 Aerosol Optical Thickness Retrievals, *J. Geophys. Res.*, *111*, D22207, doi:10.1029/2005JD006898.

Zhang, J., and J. S. Reid (2009), An analysis of clear sky and contextual biases using an operational over ocean MODIS aerosol product, *Geophys. Res. Lett.*, *36*, L15824, doi:10.1029/2009GL038723.

Zhang, J., and J. S. Reid (2010), A decadal regional and global trend analysis of the aerosol optical depth using a data-assimilation grade over-water MODIS and Level 2 MISR aerosol products, *Atmos. Chem. Phys.*, *10*, 10,949–10,963, doi:10.5194/acp-10-10949-2010.

Zhang, J., J. S. Reid, and B. N. Holben (2005), An analysis of potential cloud artifacts in MODIS over ocean aerosol optical thickness products, *Geophys. Res. Lett.*, *32*, L15803, doi:10.1029/2005GL023254.

Zhang, J., J. S. Reid, D. L. Westphal, N. L. Baker, and E. J. Hyer (2008), A system for operational aerosol optical depth data assimilation over global oceans, *J. Geophys. Res.*, *113*, D10208, doi:10.1029/2007JD009065.

Zhang, J., J. Reid, D. Westphal, E. Hyer, C. Curtis, N. Baker, J. Campbell, and P. Xian (2010), The operational aerosol data assimilation system for US Navy aerosol and visibility forecasts, paper presented at Battlespace Atmospheric and Cloud Impacts on Military Operations Conference, Air Force Weather Agency, Omaha, Nebraska, 13–15 April.

N. L. Baker, J. R. Campbell, W. F. Campbell, E. J. Hyer, J. S. Reid, and D. L. Westphal, Marine Meteorology Division, Naval Research Laboratory, 7 Grace Hopper Ave., Stop 2, Monterey, CA 93943, USA.

J. Zhang, Department of Atmospheric Science, University of North Dakota, 2901 University Ave., Stop 8264, Grand Forks, ND 58202, USA. (jzhang@atmos.und.edu)